Clinical Implications Of The Anisotropic Analytical Algorithm For IMRT Treatment Planning And Verification

Christopher M. Bragg[a,b], Katrina Wingate[a] and John Conway[a]

[a]Department of Radiotherapy Physics, Weston Park Hospital, Sheffield Teaching Hospitals NHS Foundation Trust, S10 2SJ, UK

[b]Department of Medical Physics, Faculty of Medicine, University of Sheffield, Sheffield, S10 2JF, UK

Abstract

Purpose: To determine the implications of the use of the Anisotropic Analytical Algorithm (AAA) for the production and dosimetric verification of IMRT plans for treatments of the prostate, parotid, nasopharynx and lung.
Methods: 72 IMRT treatment plans produced using the Pencil Beam Convolution (PBC) algorithm were recalculated using the AAA and the dose distributions compared. 24 of the plans were delivered to inhomogeneous phantoms and verification measurements made using a pinpoint ionisation chamber. The agreement between the AAA and measurement was determined.
Results: Small differences were seen in the prostate plans, with the AAA predicting slightly lower minimum PTV doses. In the parotid plans, there were small increases in the lens and contralateral parotid doses while the nasopharyngeal plans revealed a reduction in the volume of the PTV covered by the 95% isodose (the $V_{95\%}$) when the AAA was used. Large changes were seen in the lung plans, the AAA predicting reductions in the minimum PTV dose and large reductions in the $V_{95\%}$. The AAA also predicted small increases in the mean dose to the normal lung and the V_{20}. In the verification measurements, all AAA calculations were within 3% or 3.5mm distance to agreement of the measured doses.
Conclusions: The AAA should be used in preference to the PBC algorithm for treatments involving low density tissue but this may necessitate re-evaluation of plan acceptability criteria. Improvements to the Multi-Resolution Dose Calculation algorithm used in the inverse planning are required to reduce the convergence error in the presence of lung tissue. There was excellent agreement between the AAA and verification measurements for all sites.

Introduction

An acknowledged limitation of the correction-based commercial treatment planning system (TPS) dose calculation algorithms in wide use today is a limited ability to account for the effects of electron transport [1]. Significant errors in the calculated dose distributions often result from such algorithms' poor modelling of situations in which electronic equilibrium does not exist, in particular in the presence of inhomogeneities [2,3,4] or when small fields are used [5,6]. More recently, the introduction of convolution-superposition (CS) algorithms that better account for electron transport has enabled improved estimation of dose distributions, particularly in the absence of electronic equilibrium.

The Anisotropic Analytical Algorithm (AAA) [7], implemented in the Eclipse TPS (Varian Medical Systems, Palo Alto, Ca), is one such convolution-superposition algorithm. In common with the older photon algorithm in Eclipse, the Pencil Beam Convolution (PBC) algorithm, it considers the dose around narrow pencil beams, although the implementation is quite different. The PBC algorithm calculates the dose by convolution of a field intensity fluence with the kernel that describes dose deposition around the primary photon pencil beam in water. Inhomogeneities are accounted for by the subsequent application of corrections such as the Equivalent Tissue-Air Ratio (ETAR) correction, in which the radius of the field and the depth are scaled according to the density of the media.

By contrast, the pencil beams in the AAA include separately-modelled contributions from three sources – primary photons, extra-focal photons and contaminating electrons. Each source has associated with it a fluence, an energy deposition density function and a scatter kernel. Consideration of inhomogeneities is more intrinsic in the AAA; the scatter kernels that model lateral energy scattering are scaled anisotropically according to electron density, while the energy deposition density functions undergo density scaling in the direction of the pencil beams. The total energy deposited by each pencil beam is obtained by the convolution of the contributions from the three sources and the final dose is calculated by the superposition of the contributions from the pencil beams.

The improved accuracy of the AAA in phantom situations and 3D conformal radiotherapy (3D-CRT) treatment plans compared to Eclipse's Pencil Beam Convolution (PBC) algorithm (the Eclipse implementation of the Single Pencil Beam algorithm of the same manufacturer's CadPlan TPS) has been reported by several authors [8-12].

Intensity-modulated radiotherapy (IMRT) fields, which often comprise large numbers of small beam segments, place particular importance on the accurate modelling of small fields. Several investigations into the accuracy of a number of CS algorithms in IMRT planning [13-16] have been reported. However, there can be large differences in the abilities of different CS algorithms to model the effects of factors such as small fields and inhomogeneities [17] and so the accuracy of the AAA in calculating IMRT dose distributions cannot be inferred from the performance of other algorithms.

Sterpin *et al.* [18] compared dose distributions calculated by the AAA and Monte Carlo simulation, the current "gold standard" for dose calculation, in a phantom and for four treatment plans and found good agreement between the two, albeit with localised exceptions. They further concluded that the AAA generally provided significant improvements over the PBC algorithm.

The aim of this work was to investigate the clinical implications for IMRT treatment planning of changing from a correction-based, pencil beam dose calculation model to the AAA.

Materials and Methods

Treatment Planning

Twenty prostate treatment plans were produced, using a fixed beam arrangement with fields at gantry angles 180°, 100°, 45°, 315° and 260° (IEC1217). The prescribed dose was 60Gy in 20 fractions. The organs at risk (OARs) considered in the inverse planning process were the rectum, the bladder and the femoral heads. The tolerance doses were for no more than 50% of the bladder or rectum to receive 57Gy and no more than 2.0cm^3 of the femoral heads to receive 55Gy.

Eighteen head and neck plans were produced, nine for the treatment of parotid tumours and nine for nasopharyngeal tumours. The parotid plans, for which the prescription dose was 60Gy in 30 fractions used the five-field class solution developed in a previous study [21]. The OARs for which dose-volume constraints were specified in the inverse planning were the brain, spinal cord, contralateral parotid and lenses. The tolerance for the contralateral parotid was a mean dose of 26Gy [22,23]. The prescription doses for the nasopharyngeal plans were 50.4Gy in 1.8Gy fractions (one patient), 60Gy in 2Gy fractions (four patients) or 70Gy in 2Gy fractions (four patients). All plans used five fields, although the gantry angles used and the considered OARs varied according to the size and location of the PTV. The tolerance doses used were: brainstem and spinal cord 44Gy, brain no more than 10% receiving 55Gy, optic nerves and chiasm 50Gy and lenses 4Gy.

Finally, thirty-six non-small cell lung cancer (NSCLC) treatment plans were produced using the CHART fractionation (54Gy in 36 fractions). As the PTV locations varied widely, the beam angles were optimised for each patient. Two plans required seven fields to produce acceptable dose distributions; all others used five fields. The inverse planning aimed to maximise PTV coverage while minimising the dose received by lung tissue outside the PTV and not exceeding the tolerance dose of 44Gy for the spinal cord used clinically at this centre.

All dMLC IMRT treatment plans were produced using Eclipse, with version 7.5.18 of the Dose Calculation Server. Inverse planning was performed with the Dose-Volume Optimiser (DVO) algorithm, which employs a convolution-superposition algorithm, the Multi-Resolution Dose Calculation (MRDC) algorithm, to estimate the dose following each iteration of the optimisation process. The aim of the inverse planning was to meet the recommendations in ICRU Report 62 [24] for target coverage of between 95% and 107% of the prescription dose while minimising the doses to the OARs. (The PTV constraints set at the start of each optimisation were tighter than this, as has been found to be necessary with the DVO in order to encourage conformation to the ICRU recommendations. Constraints were interactively adjusted during each optimisation as required in order to improve the final distribution.)

The final, forward dose calculations were performed using the PBC algorithm with ETAR inhomogeneity correction and subsequently with the AAA with inhomogeneity correction, using a 2.5mm calculation grid. The choice of algorithm influenced only the forward dose calculation from the pre-determined MLC leaf movements. Each PBC plan was normalised such that the mean dose to the PTV was equal to the prescription dose; the same monitor units were set for the corresponding AAA plan.

The quality of each treatment plan was analysed with regard to its clinical acceptability. Any implications for treatment planning practice of the choice of algorithm were considered. Dose-Volume Histograms (DVHs) were produced for all plans and from them, the doses to the PTV and OARs were analysed.

PTV doses were compared in terms of the minimum and maximum doses and the percentage volume of the PTV receiving a dose greater than 95% of the prescription dose, $V_{95\%}$. Clinically-relevant OAR dose parameters were compared. For the prostate plans, these were the maximum bladder, rectum and femoral head doses, as well as the percentage volume of the bladder and rectum receiving 80% of the prescription dose ($V_{80\%}$). For the NSCLC plans, the maximum dose to the spinal cord as well as the mean dose to the non-GTV lung (hereafter referred to as “normal lung”) and the percentage volume of the normal lung receiving at least 20Gy (V_{20}) [25] were considered. For the parotid plans, the

parameters compared were the maximum brain, spinal cord and lens doses and the mean dose to the contralateral parotid gland. For the nasopharyngeal plans, there was some variation in the involved OARs between patients. The parameters studied were the maximum spinal cord dose for all patients and, where involved, the maximum brain, lens, optic nerve and optic chiasm doses.

In addition, a Conformity Index (CI) [26] was used to quantify the degree to which the high dose region was conformed to the PTV. The CI takes both the volume of PTV and the volume of normal tissue receiving at least 95% of the prescription dose into account and was calculated as the product of two parameters. The first parameter was the fraction of the PTV that received at least 95% of the prescription dose level, (V_{PTV95} / V_{PTV}). The second parameter was the ratio of V_{PTV95} to the total volume of tissue receiving at least 95% of the prescription dose (that is, the treated volume, V_T). Therefore, the CI was calculated as follows:

$$CI = \frac{V_{PTV\,95}}{V_{PTV}} \frac{V_{PTV\,95}}{V_T}$$

A CI equal to unity indicates exact conformation of the 95% isodose to the PTV, with no tissue outside the PTV receiving this dose, while a CI of zero indicates a geographical miss.

The statistical significance of differences between the dose parameters from the two algorithms was calculated using a paired, two-tailed Student's t-test.

Verification

The accuracy of the dose distributions calculated by the AAA in terms of their agreement with in-phantom verification measurements as typically performed prior to IMRT treatments [19,20] was assessed.

Ten prostate plans and six plans from each of the parotid, nasopharynx and lung plans were randomly chosen and transferred as verification plans, using the same dMLC files and monitor units, to CT scans (with a slice spacing of 2.5mm) of one of three semi-anthropomorphic phantoms. The phantoms (all CIRS Inc., Norfolk, VA) were a pelvic phantom containing bone-equivalent inhomogeneities (relative electron density 1.506), a head and neck phantom containing bone inhomogeneities and air gaps and a thorax phantom containing bone-equivalent and lung-equivalent (relative electron density 0.207) inhomogeneities. The dose distribution from each plan was calculated using the AAA with inhomogeneity correction and 2.5mm grid spacing. The plans were transferred to a Varian 600C linear accelerator, equipped with a 120-leaf Millennium MLC at 6MV, via the Varis record and verify system (Varian Medical Systems, Palo Alto, Ca).

The doses at a selection of reference points within the phantoms were measured using a PTW model 31016 (0.016cc) pinpoint ionisation chamber (PTW-Freiburg, Freiburg, Germany) and PTW Unidos Universal electrometer, correcting for linear accelerator output. Between three and six points were used for each plan, as shown in Table 2. The measured doses were compared to those calculated by the AAA. In instances where the discrepancy between measurement and calculation exceeded 3%, the distance to agreement between the measured and calculated doses was determined on Eclipse by measuring the distance between the measurement point and the isodose corresponding to dose measured at that point.

Results

Treatment Planning

Example DVHs for a prostate plan, a nasopharynx plan and a lung plan are shown in Figure 1. The results of the comparison of the IMRT treatment plans as calculated by the two algorithms are shown in Table 1.

In the prostate plans, the AAA predicted lower doses than the PBC algorithm, including slightly lower coverage by the 95% isodose. However, of those differences that were

statistically significant, only the reduction of 0.6% in the minimum PTV dose was of any clinical significance. A similar pattern was seen in the parotid plans, the only significant differences between the algorithms being the increases in the contralateral parotid and lens doses, although these were of limited clinical significance.

The PTV dose distributions in the nasopharyngeal plans were generally less ideal than in either the parotid or prostate plans, with much higher inter-patient variability in the maximum and minimum PTV doses and significantly poorer coverage of the target. The AAA predicted a slightly lower maximum dose to the brain but, more crucially, a reduction of approximately 5% of the PTV receiving 95% of the prescription dose. The lens doses from both algorithms were high as a result of a clinical decision to compromise them to avoid further reductions in target coverage.

The lung plans showed a markedly different pattern. The AAA predicted slightly lower minimum PTV doses, and a reduction of 9% of the volume of the PTV covered by the 95% isodose. Changes in the spinal cord and lung doses were smaller and of limited clinical significance. The poorer coverage of the PTV was reflected in the conformity index, which was significantly lower when the AAA was used to calculate the dose distribution.

Verification

The results of the phantom verification measurements are shown in Table 2. The reproducibility of the measurements was estimated by performing the measurements for the first plan of each treatment site five times, setting the equipment up anew between measurements and was found to be 0.3% for the measurements in the thorax and head and neck phantom and 0.5% in the pelvic phantom.

The agreement between measurement and calculation for the prostate and head and neck plans was excellent, with no discrepancy exceeding 3% or (in regions of high dose gradient) 1.6mm distance to dose agreement. The agreement for the lung and nasopharynx plans was slightly worse, the maximum discrepancies being 3% or 3.5mm (but for both sites, a single point was outside 3% or 3mm).

The AAA tended to overestimate the doses at the measurement points, the mean discrepancy over all measurements being 1.0%. The measurements in the lung-equivalent region of the thorax phantom showed small mean underestimates. However, the inter-patient variability in the discrepancies limit the conclusions that can be drawn from these observations.

Discussion

If the AAA is taken to provide a more accurate representation of the dose distribution from a given treatment, the comparisons between the AAA and PBC dose distributions in Table 1 provide an indication of the difference between the dose predicted by the PBC algorithm and that actually delivered.

In the prostate plans, the distributions were found to be very similar, with no differences between the OAR doses that were considered clinically significant. In all but three patients, the AAA predicted a lower minimum PTV dose than the PBC, with a mean reduction of 0.6% of the prescription dose. However, the two algorithms predicted virtually identical values of $V_{95\%}$ and the mean value of the minimum PTV dose was above the ICRU-recommended level of 95% (only four patients falling below this value). The parotid plans showed even greater agreement between the algorithms than the prostate plans, with no clinically significant differences.

That the differences between the algorithms' dose distributions for these plans were so small was largely due to two factors. Firstly, the beams used for these plans were such that there was little involvement of heterogeneities. The prostate fields were angled such that they avoided most of the bony anatomy of the pelvic region, while only two of the parotid beams passed through inhomogeneities, one of them being the field contralateral to the PTV whose

typical contribution to the total PTV dose was proportionately lower than the other fields. As a result, the effects of the two algorithms' abilities to account for inhomogeneities on the final dose distribution was restricted. Secondly, as each field's fluence exhibited a relatively low level of intensity modulation, each largely comprised a single MLC opening whose size evolved but had an equivalent square size of between 5 and 10cm for all but the first and last few seconds of the delivery. (This is broadly analogous to the use of a small number of large beam segments rather than a very high number of much smaller segments in a multiple static segments delivery.) Therefore, as the open part of the field at any time during the delivery was relatively large, any differences in the algorithms' ability to handle small field segments did not have a large influence on the dose distributions.

The lenses and femoral heads were outside the main fields in most instances. Therefore, the differences in the doses to those structures, in the most part, resulted from differences in the modelling of the transmission through the MLC and of the dose beyond the penumbra. The higher doses outside the field seen with the AAA are consistent with those reported for open fields by Fogliata *et al.* [8].

The verification measurements on the pelvic phantom demonstrated the accuracy of the AAA. The mean discrepancies between the calculated and measured doses at all measurement points were no greater than 1.2%. The discrepancies for several individual measurements were somewhat higher, up to 6.3%, whenever the dose discrepancy exceeded 3%, the measurement point was in a high dose gradient and the distance to dose agreement was no greater than 1.2mm. The agreement between the AAA and measurement for the parotid plans was similarly to within 3% or 1.1mm distance to agreement. The larger mean discrepancy seen at the Anterior point was again the result of the point's location in a high dose gradient for most of the plans; all measurements here were within 2.5% or 1.1mm distance to agreement.

The close proximity of OARs to the PTVs (as well as the considerably greater size of the PTVs) in the nasopharyngeal plans led to less uniform field fluences than in the parotid plans and necessitated compromises in the PTV and/or OAR doses in some patients. This was reflected in the plans' PTV coverage and the higher inter-patient variations based on the PBC-calculated distributions in many of the dose parameters studied. In some plans, clinical decisions were made to exceed OAR tolerances (most commonly with the lenses or where OARs lay within the PTV) rather than further compromise the PTV coverage. In only one of these patients did using the AAA cause an OAR (a lens) whose maximum dose was within tolerance according to the PBC algorithm to rise above tolerance and in no instance was the difference between the two algorithms large enough that a different decision would have been made on the basis of the AAA-calculated distribution.

The less uniform fluences in these plans than were required for the prostate and parotid plans resulted in a reduction in the size of the MLC openings throughout the field deliveries. The agreement between the doses calculated by the AAA plans and measurement on the head and neck phantom was less good for these nasopharynx plans. The highest discrepancies were seen at the Posterior point, outside the high dose region, although all measurements there agreed with the AAA doses to within 2.1% or 1.3mm distance to agreement. Only for one measurement (at the Right measurement point) did the level of agreement exceed 3% or 3mm, a commonly-used action level for IMRT verification [20,27]. The agreement between the AAA and measurement was comparable to that reported between other CS algorithms and measurement or Monte Carlo simulation [13-16].

Similar levels of agreement were seen for the lung plans, measured on the thorax phantom. All calculated doses agreed with measurement to within 3% or 3.3mm distance to agreement and all but one to within 3% or 3mm, confirming the accuracy of the AAA calculations of these IMRT plans. The magnitudes of the mean discrepancies were of the same order as were found in a previous study for conventional radiotherapy treatment fields measured on the thorax phantom [9] and as those reported for IMRT fields by Khodri *et al.* [28].

In the lung plans, all the OAR dose parameters investigated were found to be higher when calculated with the AAA than had been predicted by the PBC algorithm. However, the differences were not clinically significant and it should be noted that even the AAA-calculated values remained within tolerance for every plan, with the single exception of one plan's V_{20}, which exceeded the tolerance of 35% even for the PBC algorithm. However, it was, perhaps, in the PTV coverage that the most significant issues arose.

The ICRU recommendations state that the dose to the PTV should lie within 95% to 107% of the prescription dose. There was no significant difference in the maximum PTV dose when the plans were recalculated with the AAA. However, there was a large mean reduction in the minimum PTV dose of 4% and a reduction of 9% in the volume of the PTV covered by the 95% isodose. These – as with the increase in lung dose and deterioration in the conformity – were the result of the broadening of the penumbra caused by the AAA's improved modelling of the lateral electron transport and was worse for those patients whose PTV contained a large amount of lung tissue, such as the example shown in Figure 2.

There are clear discrepancies between the final PTV DVH predicted by the MRDC at the end of the inverse planning and that from the AAA, suggesting that the convolution-superposition-based MRDC is insufficiently capable of predicting the effects of low density tissue with sufficient accuracy to fully enable accurate convergence to the required dose constraints. The production of IMRT plans within the ICRU recommended PTV dose limits for the lung region, at least using the standard inverse planning methods employed in this work, is unlikely to be a realistic possibility. This raises the issue of whether the prescribed dose should be adjusted in light of the improved knowledge of the delivered distribution.

On one hand, it could be argued that the PTV coverage being lower than originally thought might necessitate an increase in the prescribed dose in order to ensure that the PTV is covered to the extent that the PBC algorithm predicted. This would be very much dependent upon the acceptance criteria used in treatment plan evaluation. For example, if the requirement were for the mean PTV dose to be equal to the prescription dose, the required increase in the instances studied here would not be large. The mean MU would be increased by 1.3% for the nasopharyngeal plans and by less than 1% for the other sites. Table 3 shows the corresponding dose parameters following renormalisation of the AAA plans such that the mean PTV dose was equal to the prescription dose (while the mean changes in monitor units involved in the renormalisation for each site are shown in Table 4). As can be seen, the differences between the original AAA plans and the renormalised plans small and so the implications of such a change would be limited. However, clinically significant reductions in PTV coverage in the NSCLC plans remain. To alter the AAA plans such that an equivalent degree of coverage, for example, in terms of the fraction of the PTV covered by the 95% isodose, were achieved would require much larger increases in monitor units.

On the other, current clinical experience of treatment outcomes are correlated with the doses as predicted by less accurate algorithms. To alter treatment regimes solely on the basis of improved dose calculation accuracy would have wide ranging implications particularly in terms of normal tissue reactions. The treatment of NSCLC by radiotherapy has higher associated uncertainties than most radiotherapy treatments, due to factors such as the particularly significant tumour motion and poor prognoses of patients; to increase doses purely on the basis of improved knowledge of the dose distributions would be to introduce a further source of uncertainty into the radiotherapy process. Of paramount importance in making the clinical decision as to whether a treatment regime should be so altered is the development of more accurate dose-effect relationships than are currently available; the more accurate knowledge of the doses afforded by improved calculation algorithms is vital to this end.

Conclusions

The AAA was, in general, not found to significantly alter the quality of IMRT treatment plans for the prostate, parotid or nasopharynx compared to the PBC algorithm. However, some

small differences were seen and the importance of evaluating treatment plans on an individual basis cannot be overemphasised. The PBC algorithm overestimated the PTV coverage in IMRT plans for NSCLC, the AAA's more accurate modelling of lateral electron transport demonstrating significant increases in the volume of the PTV being underdosed. The use of the AAA in preference to the PBC algorithm for treating planning in which low density tissue such as lung is present is recommended, although improvements to the MRDC algorithm are required for IMRT treatments to benefit fully from its improved accuracy. The differences between the algorithms were of similar magnitude to those previously found for conventional plans. Excellent agreement between the AAA and verification measurements using a pinpoint ionisation chamber in inhomogeneous phantoms was seen, the majority of calculated doses agreeing with measurement to within 3% or 3mm distance to agreement.

References

[1] Arnfield, M.R., Siantar, C.H., Siebers, J., Garmon, P., Cox, L. and Mohan, R. The impact of electron transport on the accuracy of computed dose. Med Phys 2000;27:1266-1274.

[2] Carrasco P, Jornet N, Duch MA *et al.* Comparison of dose calculation algorithms in phantoms with lung equivalent heterogeneities under conditions of lateral electronic disequilibrium. Med Phys 2004;31:2899-2911.

[3] Shahine BH, Al-Ghazi MSAL and El-Khatib E. Experimental evaluation of interface doses in the presence of air cavities compared with treatment planning algorithms. Med Phys 1999;26:350-355.

[4] American Association of Physicists in Medicine. Tissue inhomogeneity corrections for megavoltage photon beams, AAPM Report 85. New York: AAPM, 2004.

[5] Jones AO and Das IJ. Comparison of inhomogeneity correction algorithms in small photon fields. Med Phys 2005;32:766-776.

[6] Sandilos P, Seferlis S, Antypas C, Karaiskos P, Dardoufas C and Vlahos L. Technical Note: Evaluation of dosimetric performance in a commercial 3D treatment planning system. Br J Radiol 2005;78:899-905.

[7] Ulmer W, Pyyry J and Kaissl W. A 3D Photon superposition/convolution algorithm and its foundation on results of Monte Carlo calculations. Phys Med Biol 2005;50:1767-1790.

[8] Fogliata A, Nicolini G, Vanetti E, Clivio A and Cozzi L. Dosimetric validation of the anisotropic analytical algorithm for photon dose calculation: fundamental characterization in water. Phys Med Biol 2006;51:1421-38.

[9] Bragg CM and Conway J. Dosimetric verification of the Anisotropic Analytical Algorithm for radiotherapy treatment planning. Radiother Oncol 2006;81:315-323.

[10] Knoos T, Wieslander E, Cozzi L et al. Comparison of dose calculation algorithms for treatment planning in external photon beam therapy for clinical situations. Phys Med Biol 2006;51:5785-5807.

[11] Fogliata A, Vanetti E, Albers D et al. On the dosimetric behaviour of photon dose calculation algorithms in the presence of simple geometric heterogeneities: comparison with Monte Carlo calculations. Phys Med Biol 2007;52:1363-1385.

[12] Van Esch A, Tillikainen L, Pyykkonen J et al. Testing of the Analytical Anisotropic Algorithm for photon dose calculation. Med Phys 2006;33:4130-4148.

[13] Mihaylov I, Lerma F and Siebers J. Comparison of Monte Carlo and convolution/superposition calculation methods: quantification of the dose prediction errors arising from tissue heterogeneities. Med Phys 2005;32:1901-1902.

[14] Francescon P, Cora S and Chiovati P. Dose verification of an IMRT treatment planning system with the Beam EGS4-based Monte Carlo code. Med Phys 2003;30:144-157.

[15] Partridge M, Trapp JV, Adams EJ, Leach MO, Webb S and Seco J. An investigation of dose calculation accuracy in intensity-modulated radiotherapy of sites in the

head & neck. Phys Med 2006;22:97-104.

[16] Al-Hallaq HA, Reft CS and Roeske JC. The dosimetric effects of tissue heterogeneities in intensity-modulated radiation therapy (IMRT) of the head and neck. Phys Med Biol 2006;51:1145-1156.

[17] Vanderstraeten B, Reynaert N, Paelinck L et al. Accuracy of patient dose calculation for lung IMRT: a comparison of Monte Carlo, convolution/superposition, and pencil beam computations. Med Phys 2006;33:3149-3158.

[18] Sterpin E, Tomsej M, De Smedt B, Reynaert N and Vynckier S. Monte Carlo evaluation of the AAA treatment planning algorithm in a heterogeneous multilayer phantom and IMRT clinical treatments for an Elekta Sl25 Linear Accelerator. Med Phys 2007;34:1665-1677.

[19] Sandilos P, Angelopoulos A, Baras P et al. Dose verification in clinical IMRT prostate incidents. Int J Rad Onc Biol Phys 2004;59:1540-1547.

[20] Nelms BE and Simon JA. A survey on IMRT QA analysis. J Appl Clin Med Phys 2007;8:76-90.

[21] Bragg CM, Conway J and Robinson MH. The role of intensity-modulated radiotherapy in the treatment of parotid tumors. Int J Rad Onc Biol Phys 2002;52:729-738.

[22] Blanco AI, Chao KSC, El Naqa I et al. Dose-Volume Modeling of Salivary Function in Patients With Head-and-Neck Cancer Receiving Radiotherapy. Int J Rad Onc Biol Phys 2005;62:1055-1069.

[23] Eisbruch A, Ten Haken RK, Kim HM, Marsh LH and Ship JA. Dose, Volume, and Function Relationships in Parotid Salivary Glands Following Conformal and Intensity-Modulated Irradiation of Head and Neck Cancer. Int J Rad Onc Biol Phys 1999;45:577-587.

[24] International Commission on Radiation Units and Measurements (ICRU) Report 62. Prescribing, recording, and reporting photon beam therapy (supplement to ICRU Report 50). Bethesda, MD: ICRU Publications; 1999.

[25] Rodrigues G, Lock M, d'Souza D, Yu E and Van Dyk J. Prediction of Radiation Pneumonitis by Dose-Volume Histogram Parameters in Lung Cancer - a Systematic Review. Radiother Oncol 2004;71:127-138.

[26] Van't Riet A, Mak ACA, Moerland MA, Elders LH and Vanderzee W. A conformation number to quantify the degree of conformality in brachytherapy and external beam irradiation: application to the prostate. Int J Rad Onc Biol Phys 1997;37:731-736.

[27] Budgell GJ, Perrin BA, Mott JHL, Fairfoul J and Mackay RI. Quantitative Analysis of Patient-Specific Dosimetric Imrt Verification. Phys Med Biol 2005;50:103-119.

[28] Khodri M, Plattard D, Martin H et al. On the Clinical and Dosimetric Accuracy of Anisotropic Analytical Algorithm Photon Dose Calculation in the Case of Lung Inhomogeneities for IMRT Treatment. Int J Rad Onc Biol Phys 2007;69:S716

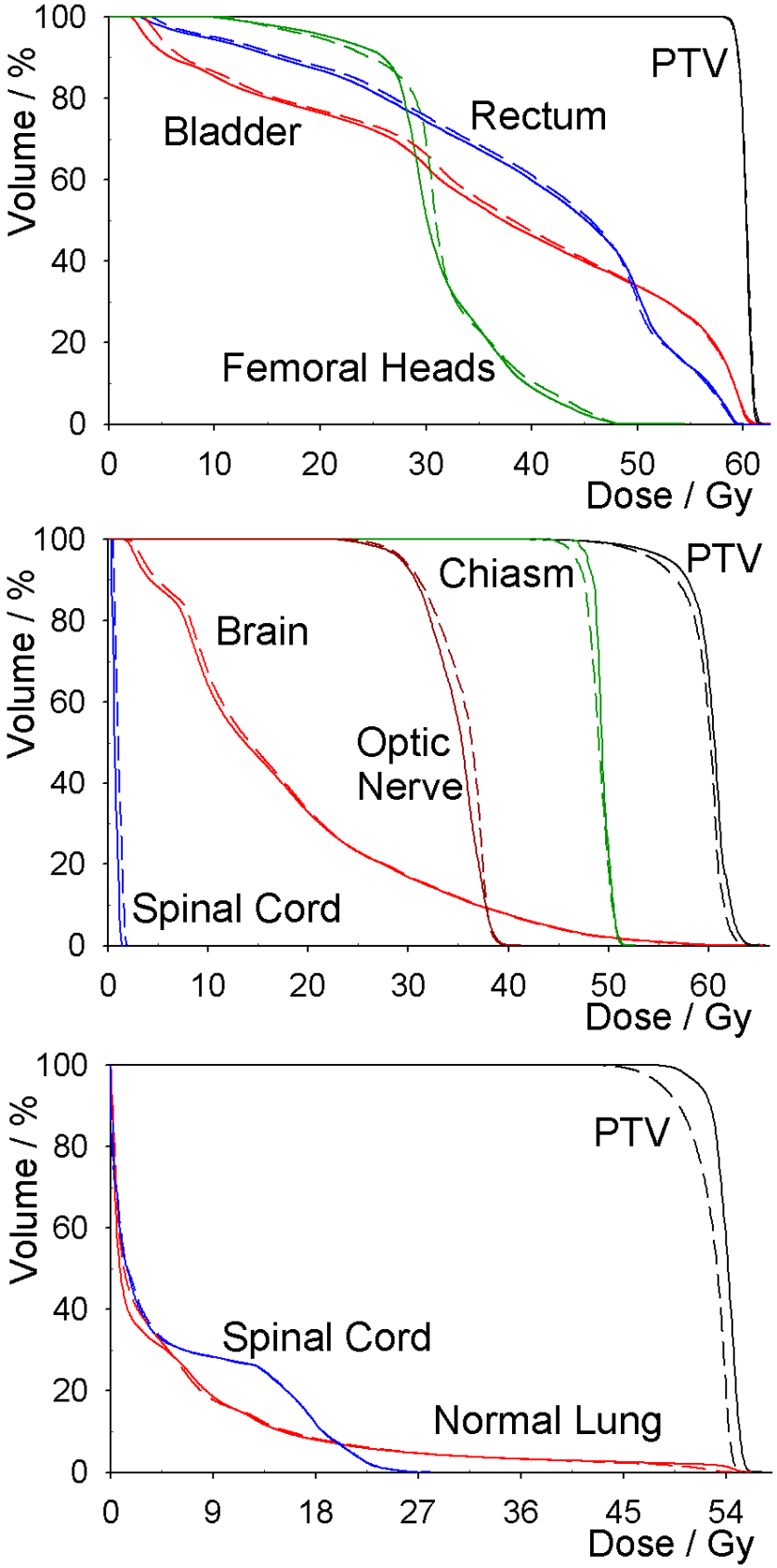

Fig. 1 Example DVHs for (top) a prostate plan, (middle) a nasopharynx plan and (bottom) a lung plan. The solid lines are the curves calculated by the PBC algorithm and the dashed lines are those calculated by the AAA

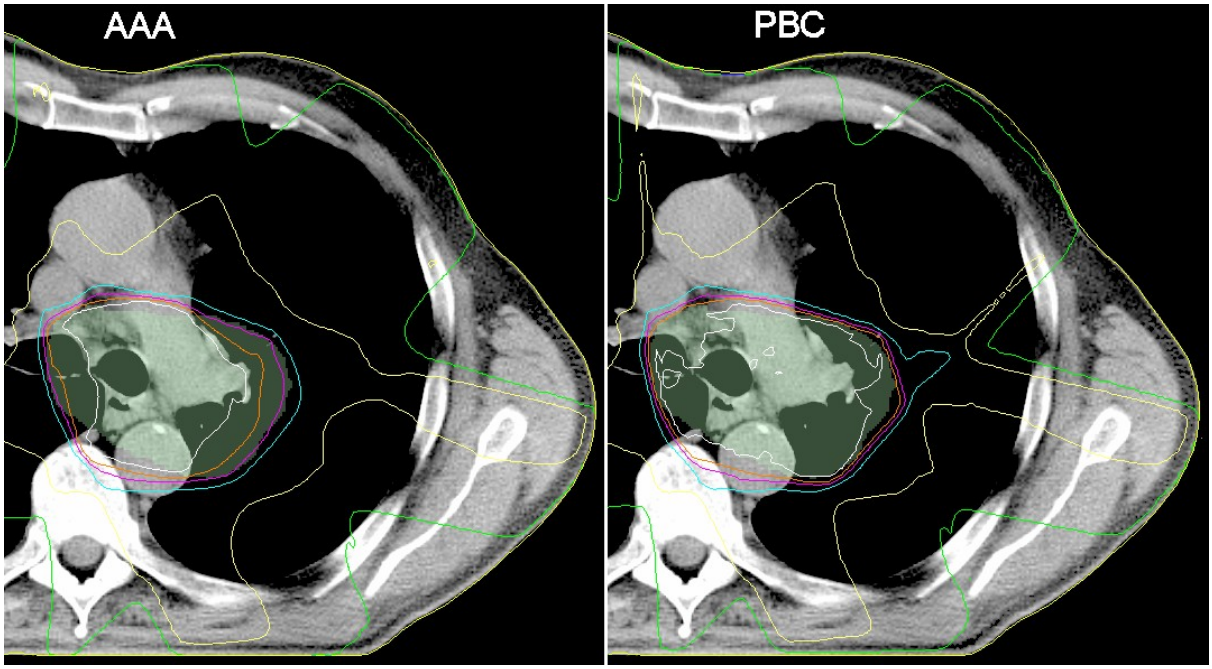

Fig. 2 An axial slice showing a representative comparison between the AAA and PBC algorithm distributions. The PTV is shaded. The isodoses displayed are 100%, 95%, 90%, 80%, 50% and 20%. The broadening of the penumbra can be seen, particularly to the lateral side of the PTV.

Table 1 Summary of differences between the treatment plan parameters from the two algorithms

Site	Volume	Parameter	AAA		PBC		p
			Mean	SD	Mean	SD	
Prostate	PTV	D_{min} (%)	95.5	1.8	96.1	2.0	0.001
		D_{max} (%)	100.9	1.0	101.9	0.7	0.000
		$V_{95\%}$ (%)	99.9	0.3	100.0	0.1	0.28
	Rectum	D_{max} (Gy)	58.3	0.9	58.8	0.9	0.000
		$V_{80\%}$ (%)	25.1	11.1	25.8	11.1	0.010
	Bladder	D_{max} (Gy)	59.7	0.4	60.1	0.3	0.000
		$V_{80\%}$ (%)	16.6	7.0	16.7	7.0	0.019
	Femoral heads	D_{max} (Gy)	37.2	5.4	37.0	5.5	0.000
		CI	0.63	0.05	0.60	0.05	0.000
Parotid	PTV	D_{min} (%)	85.2	3.6	84.2	4.9	0.30
		D_{max} (%)	103.6	1.7	103.6	1.3	0.91
		$V_{95\%}$ (%)	98.0	1.0	98.5	1.0	0.13
	Spinal Cord	D_{max} (Gy)	40.8	4.2	41.0	4.3	0.52
	Brain	D_{max} (Gy)	28.1	6.1	28.0	6.2	0.46
	C/L Parotid	D_{mean} (Gy)	16.5	1.4	15.8	1.4	0.000
	Lenses	D_{max} (Gy)	2.0	0.7	1.0	0.3	0.000
		CI	0.80	0.05	0.79	0.07	0.20
Nasopharynx	PTV	D_{min} (%)	56.3	17.7	55.2	21.0	0.71
		D_{max} (%)	109.2	2.4	110.2	2.8	0.05
		$V_{95\%}$ (%)	77.8	22.9	82.5	23.3	0.015
	Spinal Cord	D_{max} (Gy)	35.7	14.1	36.1	14.4	0.15
	Brain	D_{max} (Gy)	52.6	9.5	53.5	9.8	0.038
	Chiasm	D_{max} (Gy)	43.5	16.8	44.3	17.3	0.06
	Optic Nerves	D_{max} (Gy)	50.7	7.4	51.0	6.4	0.67
	Lenses	D_{max} (Gy)	12.7	11.2	10.3	11.3	0.000
		CI	0.68	0.19	0.69	0.19	0.41
Lung	PTV	D_{min} (%)	74.8	5.2	78.8	5.8	0.000
		D_{max} (%)	108.2	3.3	108.3	3.6	0.99
		$V_{95\%}$ (%)	88.2	5.6	97.2	2.0	0.000
	Spinal Cord	D_{max} (Gy)	36.4	8.5	35.6	8.1	0.000
	Normal Lung	D_{mean} (Gy)	12.4	3.7	12.1	3.6	0.000
		V_{20} (%)	23.2	8.5	22.7	8.3	0.001
		CI	0.67	0.06	0.83	0.09	0.000

Table 2 Summary of the IMRT verification measurements for the four treatment sites

Site	Measurement Point	Discrepancy (AAA – measured) / %		Comments
		Mean	SD	
Prostate	Isocentre	0.0	0.7	All measurements within 3% or
	Ant	1.2	0.8	1.6mm distance to agreement
	Post	1.0	2.3	
	Right	1.2	1.1	
	Left	0.7	0.6	
Parotid	Isocentre	0.9	0.6	All measurements within 3% or
	Ant	-1.9	3.6	1.1mm distance to agreement
	Post	1.1	2.3	
Nasopharynx	Isocentre	1.8	3.2	All measurements within 3% or
	Right	2.0	2.9	3.5mm distance to agreement
	Left	-0.4	2.8	
	Post	3.6	6.8	
Lung	Mediastinal_1	2.2	1.9	All measurements within 3% or
	Mediastinal_2	2.0	1.4	3.3mm distance to agreement
	Mediastinal_3	1.7	1.2	
	Mid Left Lung	-0.9	3.7	
	Post Left Lung	-0.6	3.0	
	Spinal Cord	2.6	2.7	

Table 3 Summary of differences between the treatment plan parameters from the two algorithms after renormalisation of the AAA plans

Site	Volume	Parameter	AAA		PBC		p
			Mean	SD	Mean	SD	
Prostate	PTV	D_{min} (%)	96.2	1.8	96.1	2.0	0.36
		D_{max} (%)	101.6	0.8	101.9	0.7	0.001
		$V_{95\%}$ (%)	100.0	0.2	100.0	0.1	0.34
	Rectum	D_{max} (Gy)	58.8	0.9	58.8	0.9	0.69
		$V_{80\%}$ (%)	26.4	11.2	25.8	11.1	0.003
	Bladder	D_{max} (Gy)	60.2	0.3	60.1	0.3	0.22
		$V_{80\%}$ (%)	17.0	7.1	16.7	7.0	0.000
	Femoral heads	D_{max} (Gy)	37.4	5.4	37.0	5.5	0.000
		CI	0.59	0.06	0.60	0.05	0.34
Parotid	PTV	D_{min} (%)	85.8	3.8	84.2	4.9	0.09
		D_{max} (%)	104.3	1.4	103.6	1.3	0.15
		$V_{95\%}$ (%)	98.7	0.7	98.5	1.0	0.47
	Spinal Cord	D_{max} (Gy)	41.0	4.1	41.0	4.3	0.84
	Brain	D_{max} (Gy)	28.3	6.1	28.0	6.2	0.015
	C/L Parotid	D_{mean} (Gy)	16.6	1.4	15.8	1.4	0.000
	Lenses	D_{max} (Gy)	2.0	0.7	1.0	0.3	0.000
		CI	0.79	0.06	0.79	0.07	0.29
Nasopharynx	PTV	D_{min} (%)	57.2	18.2	55.2	21.0	0.48
		D_{max} (%)	110.7	1.8	110.2	2.8	0.27
		$V_{95\%}$ (%)	83.0	20.3	82.5	23.3	0.71
	Spinal Cord	D_{max} (Gy)	36.3	14.4	36.1	14.4	0.48
	Brain	D_{max} (Gy)	53.3	9.4	53.5	9.8	0.57
	Chiasm	D_{max} (Gy)	44.1	17.0	44.3	17.3	0.52
	Optic Nerves	D_{max} (Gy)	51.5	7.5	51.0	6.4	0.48
	Lenses	D_{max} (Gy)	12.8	11.2	10.3	11.3	0.000
		CI	0.70	0.16	0.69	0.19	0.76
Lung	PTV	D_{min} (%)	75.5	5.8	78.8	5.8	0.000
		D_{max} (%)	108.6	2.6	108.3	3.6	0.30
		$V_{95\%}$ (%)	90.0	2.7	97.2	2.0	0.000
	Spinal Cord	D_{max} (Gy)	36.4	8.2	35.6	8.1	0.000
	Normal Lung	D_{mean} (Gy)	12.4	3.6	12.1	3.6	0.000
		V_{20} (%)	23.2	8.3	22.7	8.3	0.000
		CI	0.77	0.08	0.83	0.09	0.000

Table 4 Summary of the monitor unit (MU) changes resulting from renormalisation of the AAA plans. Positive values indicate increased MU after renormalisation, expressed as a percentage of the PBC-calculated MU.

Site	Δ_{MU} (%)		p
	Mean	SD	
Prostate	0.8	0.5	0.000
Parotid	0.7	0.7	0.02
Nasopharynx	1.3	0.8	0.002
Lung	0.4	1.2	0.08